

*ARMY RESEARCH LABORATORY*



**CTH Analyses of Fragment Penetration  
Through Heat Sink Fins**

**by Anand Prakash**

**ARL-TR-3535**

**June 2005**

## **NOTICES**

### **Disclaimers**

The findings in this report are not to be construed as an official Department of the Army position unless so designated by other authorized documents.

Citation of manufacturer's or trade names does not constitute an official endorsement or approval of the use thereof.

**DESTRUCTION NOTICE**—Destroy this report when it is no longer needed. Do not return it to the originator.

# **Army Research Laboratory**

Aberdeen Proving Ground, MD 21005-5068

---

**ARL-TR-3535**

**June 2005**

---

## **CTH Analyses of Fragment Penetration Through Heat Sink Fins**

**Anand Prakash**  
Survivability/Lethality Analysis Directorate, ARL

REPORT DOCUMENTATION PAGE			Form Approved OMB No. 0704-0188		
Public reporting burden for this collection of information is estimated to average 1 hour per response, including the time for reviewing instructions, searching existing data sources, gathering and maintaining the data needed, and completing and reviewing the collection information. Send comments regarding this burden estimate or any other aspect of this collection of information, including suggestions for reducing the burden, to Department of Defense, Washington Headquarters Services, Directorate for Information Operations and Reports (0704-0188), 1215 Jefferson Davis Highway, Suite 1204, Arlington, VA 22202-4302. Respondents should be aware that notwithstanding any other provision of law, no person shall be subject to any penalty for failing to comply with a collection of information if it does not display a currently valid OMB control number. <b>PLEASE DO NOT RETURN YOUR FORM TO THE ABOVE ADDRESS.</b>					
1. REPORT DATE (DD-MM-YYYY) June 2005		2. REPORT TYPE Final		3. DATES COVERED (From - To) 2003 to 2005	
4. TITLE AND SUBTITLE  CTH Analyses of Fragment Penetration Through Heat Sink Fins			5a. CONTRACT NUMBER		
			5b. GRANT NUMBER		
			5c. PROGRAM ELEMENT NUMBER		
6. AUTHOR(S)  Anand Prakash (ARL)			5d. PROJECT NUMBER AH80		
			5e. TASK NUMBER		
			5f. WORK UNIT NUMBER		
7. PERFORMING ORGANIZATION NAME(S) AND ADDRESS(ES) U.S. Army Research Laboratory Survivability/Lethality Analysis Directorate Aberdeen Proving Ground, MD 21005-5068			8. PERFORMING ORGANIZATION REPORT NUMBER  ARL-TR-3535		
9. SPONSORING/MONITORING AGENCY NAME(S) AND ADDRESS(ES)			10. SPONSOR/MONITOR'S ACRONYM(S)		
			11. SPONSOR/MONITOR'S REPORT NUMBER(S)		
12. DISTRIBUTION/AVAILABILITY STATEMENT  Approved for public release; distribution is unlimited.					
13. SUPPLEMENTARY NOTES					
14. ABSTRACT  Vulnerability/lethality analysis codes (e.g., MUVES-S2) generally use the FATEPEN (fast air target encounter penetration) and THOR penetration models to determine damage produced by impacts of fragments. For simple impact scenarios, e.g., normal fragment impact on monolithic plates, these two models give reasonable predictions for penetration, perforation, and residual velocity. It is, however, not clear how realistic the predictions of these models are for more complicated scenarios. This report presents more detailed calculations of the penetration and perforation of an electronic box with cooling fins by a high velocity fragment that strikes the fins with an oblique impact. We do this by conducting physics-based, three-dimensional, numerical simulations with the CTH finite difference code. It is found that the presence of fins significantly reduces the residual velocity of the fragment. Predictions of CTH for oblique impact on plain walls are also compared with those from FATEPEN and THOR.					
15. SUBJECT TERMS CTH analysis; FATEPEN; fragment; heat sink fins; impact; lethality; modeling; penetration; projectile; simulation; THOR					
16. SECURITY CLASSIFICATION OF:			17. LIMITATION OF ABSTRACT  SAR	18. NUMBER OF PAGES  30	19a. NAME OF RESPONSIBLE PERSON Anand Prakash
a. REPORT Unclassified	b. ABSTRACT Unclassified	c. THIS PAGE Unclassified			19b. TELEPHONE NUMBER (Include area code) 410-278-5687

---

## Contents

---

<b>List of Figures</b>	<b>iv</b>
<b>List of Tables</b>	<b>v</b>
<b>1. Introduction</b>	<b>1</b>
1.1 Background .....	1
1.2 Objective .....	1
<b>2. Methodology</b>	<b>1</b>
2.1 Conventional Models .....	1
2.2 The CTH Simulations.....	2
<b>3. Results of the CTH Simulations</b>	<b>3</b>
3.1 Simulation of the Actual Scenario With the Fins.....	3
3.2 Simulation Without the Fins .....	4
3.3 Simulation With Walls of Equivalent Thicknesses.....	8
<b>4. Summary and Discussion</b>	<b>13</b>
<b>5. References</b>	<b>15</b>
<b>Appendix A. CTH Input Details for the Actual Scenario With the Fins</b>	<b>17</b>
<b>Distribution List</b>	<b>21</b>

---

## List of Figures

---

Figure 1. Driver’s integrated display with vertical cooling fins on the top wall. ....	3
Figure 2. Initial state (0 $\mu\text{s}$ ) of CTH simulation of oblique impact of the projectile on the wall with fins.....	4
Figure 3. The impact at 20 $\mu\text{s}$ for the actual scenario.....	5
Figure 4. The impact at 100 $\mu\text{s}$ for the actual scenario.....	5
Figure 5. The impact at 200 $\mu\text{s}$ for the actual scenario.....	5
Figure 6. The impact at 280 $\mu\text{s}$ for the actual scenario.....	5
Figure 7. Projectile velocity as a function of time for the actual scenario.....	6
Figure 8. Initial state (0 $\mu\text{s}$ ) of CTH simulation of oblique impact of the projectile on the bare wall without fins.....	7
Figure 9. The simulation for the bare wall impact at 20 $\mu\text{s}$ . ....	7
Figure 10. The simulation for the bare wall impact at 40 $\mu\text{s}$ . ....	7
Figure 11. The simulation for the bare wall impact at 100 $\mu\text{s}$ . ....	7
Figure 12. The simulation for the bare wall impact at 200 $\mu\text{s}$ . ....	8
Figure 13. The simulation for the bare wall impact at 100 $\mu\text{s}$ . ....	8
Figure 14. Initial state (0 $\mu\text{s}$ ) of CTH simulation of oblique impact of the projectile on a wall of thickness equal to that of the bare wall plus the thickness of two fins. ....	8
Figure 15. The simulation with wall thickness increased by twice the fin thickness at 20 $\mu\text{s}$ . ....	8
Figure 16. The simulation with wall thickness increased by twice the fin thickness at 40 $\mu\text{s}$ . ....	9
Figure 17. The simulation with wall thickness increased by twice the fin thickness at 100 $\mu\text{s}$ . ....	9
Figure 18. The simulation with wall thickness increased by twice the fin thickness at 200 $\mu\text{s}$ . ....	9
Figure 19. The simulation with wall thickness increased by twice the fin thickness at 280 $\mu\text{s}$ . ....	9
Figure 20. Projectile velocity as a function of time for the case when wall thickness is increased by twice the fin thickness.....	10
Figure 21. Initial state (0 $\mu\text{s}$ ) of CTH simulation of oblique impact of the projectile on a wall of thickness equal to that of the bare wall plus the thickness of three fins.....	11
Figure 22. The simulation with wall thickness increased by three times the fin thickness at 20 $\mu\text{s}$ .....	11
Figure 23. The simulation with wall thickness increased by three times the fin thickness at 40 $\mu\text{s}$ .....	11
Figure 24. The simulation with wall thickness increased by three times the fin thickness at 100 $\mu\text{s}$ .....	11
Figure 25. The simulation with wall thickness increased by three times the fin thickness at 200 $\mu\text{s}$ .....	12
Figure 26. The simulation with wall thickness increased by three times the fin thickness at 280 $\mu\text{s}$ .....	12

Figure 27. Projectile velocity as a function of time for the case when wall thickness is increased by three times the fin thickness.....12

---

**List of Tables**

---

Table 1. Summary of residual velocity magnitudes.....12

INTENTIONALLY LEFT BLANK

---

# 1. Introduction

---

## 1.1 Background

For analyzing the survivability of crew and vehicle components on the battlefield, the vulnerability/lethality analysis code MUVES-S2 generally uses the empirical/analytical models FATEPEN (fast air target encounter penetration) and THOR (1, 2) for tracing the penetration, perforation, residual velocity, and residual mass of fragments that strike the system. For simple scenarios, such as the normal impact of a fragment-simulating projectile (FSP) on a monolithic armor plate, these models generally give sufficiently accurate predictions. For more complicated scenarios, such as the oblique impact of an FSP on complex component geometries, the response is much more complicated as well. Thus, it would be of interest to investigate the use of a physics-based finite difference code such as CTH (3) to predict the response and compare the results to FATEPEN and THOR.

## 1.2 Objective

The purpose of this project was to conduct three-dimensional (3-D) CTH analyses of an oblique impact of an FSP on an electronics box with cooling fins which has been used on the U.S. Army's Stryker vehicle. The FSP impacts obliquely on the fins (ribs) on top of the box, and the question addressed is whether the presence of fins significantly reduces the lethality of the projectile. We obtained an answer to this by conducting 3-D, numerical simulations with the CTH code using the Department of Defense's high performance computers at the U.S. Army Research Laboratory's major shared resource center. In addition, the CTH results are also compared with the predictions of the conventional algorithms, FATEPEN and THOR.

---

# 2. Methodology

---

## 2.1 Conventional Models

The vulnerability analysis code MUVES-S2 uses the models THOR and FATEPEN for fragment penetration. THOR is a semi-empirical model based on curve fitting to fairly extensive experimental data regarding the penetration of plates by projectiles. Given an initial state, THOR's algebraic equations calculate the final state. For example, the THOR equation for residual velocity is as follows.

$$V_r = V_s - \left( 10^c * [e * A]^\alpha * M_s^\beta * [Sec\{\theta\}]^\gamma * V_s^\lambda \right)$$

in which

$V_r$  = fragment residual velocity in feet per second.

$V_s$  = fragment striking velocity in feet per second.

$e$  = target thickness in inches.

$A$  = average impact area of the fragment in square inches.

$M_s$  = weight of original fragment in grains.

$\theta$  = angle between trajectory of fragment and target normal.

$c, \alpha, \beta, \gamma, \lambda$  = constants determined for each target material.

FATEPEN uses “engineering” models of terminal ballistic penetration. For core penetration models, FATEPEN makes assumptions of ideal impact geometries and applies laws of mechanics in a simplified way to the dominant terminal ballistic loading and response mechanisms; this allows FATEPEN to obtain algebraic equations relating the known initial conditions to a simplified final configuration. In both FATEPEN and THOR, one specifies the initial projectile parameters (shape, mass, and velocity, etc.) and the target parameters (plate material, thickness, etc.) and the model calculates, via several subroutines, the final state of affairs after the terminal ballistic interaction is finished.

## 2.2 The CTH Simulations

In contrast to the conventional engineering and semi-empirical models, the CTH code calculates the time development of the terminal ballistic event from “first principles.” CTH is an Eulerian finite difference code in which the differential equations of continuum mechanics are integrated over a fixed spatial mesh in small time steps to obtain the time development of the physical event. CTH has a Lagrangian first phase and a second phase that uses a mesh re-mapping to bring the distorted mesh back to the stationary Eulerian mesh by the use of a second order accurate advection scheme. The code uses experimentally determined material properties as an input in the form of material model parameters. For a thorough description of CTH, the reader is referred to the standard reference (3).

3-D simulations of an oblique impact of an FSP on an electronics box with the geometry of the driver’s panel on a Stryker vehicle were conducted with the CTH code. The physical assumptions in the CTH simulations are the material models. For the aluminum target, the simulations used the Mie-Gruneisen equation of state, with parameters from CTH library under the key word 1100-aluminum. It is known that metals are well represented by the Mie-Gruneisen equation of state. For the steel projectile of density  $7.87\text{g/cm}^2$ , the tabular equation of state for steel, given in the “sesame” data set of CTH library, was used. The first simulation was also re-run with the Mie-Gruneisen parameters of key word 304\_SS, and no appreciable differences in results were seen. For both materials, the Johnson-Cook constitutive model (4) was used. The model describes the yield surface of the material based on strain, strain rate, and temperature. The model parameters used were those in CTH library corresponding to 4340-steel and 1100-aluminum. In addition, the Johnson-Cook fracture model (5) was used for the projectile, with parameters under the key word

steel in the CTH library, and the Grady-Kipp model (6) was chosen for the target since this model was specifically developed to reproduce spall. Two sets of Grady-Kipp model parameters for aluminum are available in the CTH library; the one corresponding to the density of 1100\_aluminum was used. These models are strain rate dependent and keep track of accumulated damage in each cell over the various time steps. CTH input details for the actual scenario with the fins are shown in appendix A.

The electronics box with fins on a Stryker is the driver's integrated display (figure 1). The top panel (wall) has a thickness of 0.4 inch and it has vertical cooling fins (ribs) which are 0.75 inch high, 0.16 inch thick, with 0.24-inch air gaps. This electronics box (including the fins) is made of aluminum. The case scenario simulated is the impact of a 4340-steel FSP of mass 3.06 g, with a length-to-diameter ratio  $L/D = 1.17$ , arriving at an obliquity of 45 degrees to the top panel with a striking velocity of 1 km/s which overmatches 0.4-inch-thick aluminum. In the CTH simulations, a uniform mesh with a cell size of 0.08 cm by 0.08 cm by 0.08 cm was used. This gives five cells across a fin thickness.



Figure 1. Driver's integrated display with vertical cooling fins on the top wall.

---

### 3. Results of the CTH Simulations

---

#### 3.1 Simulation of the Actual Scenario With the Fins

The cross-sectional view of the initial state (time = 0  $\mu$ s) of the first 3-D CTH simulation is shown in figure 2. The geometry was rotated so that the top panel is vertical. The cylindrical

FSP is moving upward at 45 degrees from the lower left corner. The fins are shown in different colors in order to distinguish them as they become distorted and perforated during the impact event.

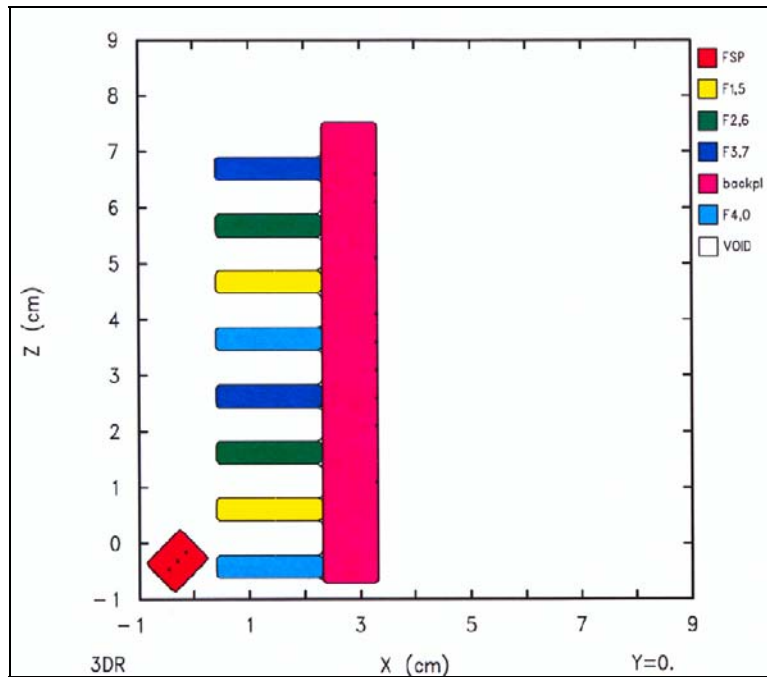


Figure 2. Initial state ( $0 \mu\text{s}$ ) of CTH simulation of oblique impact of the projectile on the wall with fins.

The next four figures (figures 3 through 6) show the time sequence of events at  $20 \mu\text{s}$ ,  $100 \mu\text{s}$ ,  $200 \mu\text{s}$ , and  $280 \mu\text{s}$ . From figure 3, we see that at  $20 \mu\text{s}$ , one fin (yellow) was perforated, and this fin is impacting the next (green) fin together with the projectile. Figure 4 shows that at  $100 \mu\text{s}$ , the third (dark blue) fin has been perforated and the FSP has nearly perforated the wall of the box (pink). Figure 5 shows the situation at  $200 \mu\text{s}$  when the FSP is moving freely after perforation with behind-armor debris (BAD) next to it. Figure 6 (at  $280 \mu\text{s}$ ) shows that the fifth fin (yellow) survives and the FSP and wall debris (pink) fly into the box. The magnitude of the FSP velocity as a function of time is plotted in figure 7. The figure shows that during the FSP's interaction with the fins and the panel wall, the velocity of the FSP rapidly falls from its initial value of  $1000 \text{ m/s}$  and, after perforation, the residual velocity magnitude settles to  $222 \text{ m/s}$ . According to CTH simulations, there is no discernible mass erosion of the FSP.

### 3.2 Simulation Without the Fins

Prior MUVES-S2 analyses involving Stryker's electronics box did not include the cooling fins. Thus, a CTH simulation of the FSP impact without the fins was also conducted and compared with the results in section 3.1.

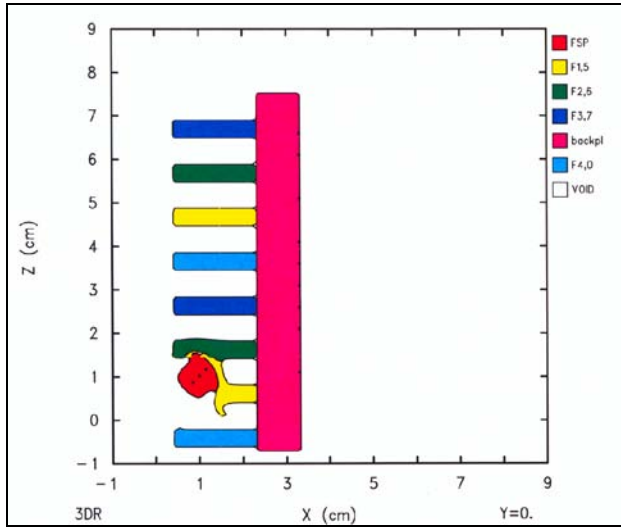


Figure 3. The impact at 20  $\mu\text{s}$  for the actual scenario.

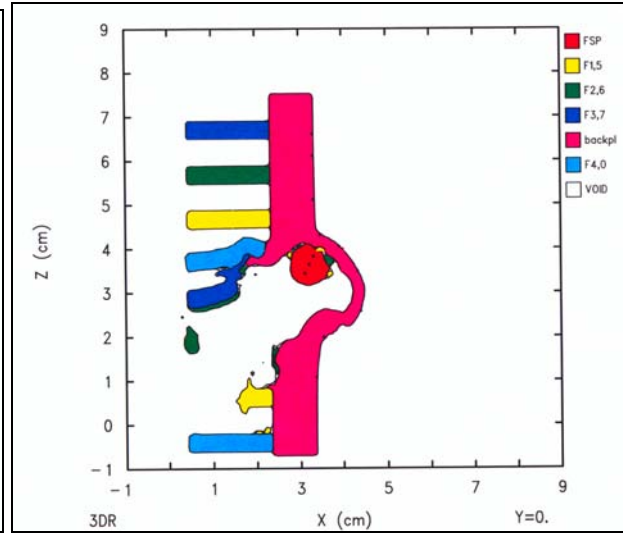


Figure 4. The impact at 100  $\mu\text{s}$  for the actual scenario.

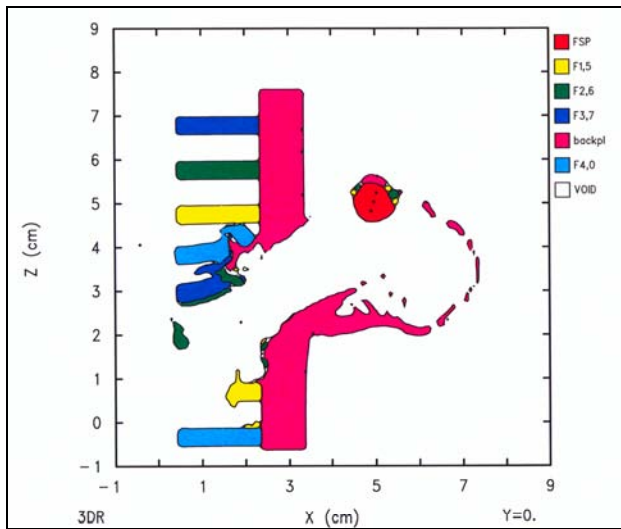


Figure 5. The impact at 200  $\mu\text{s}$  for the actual scenario.

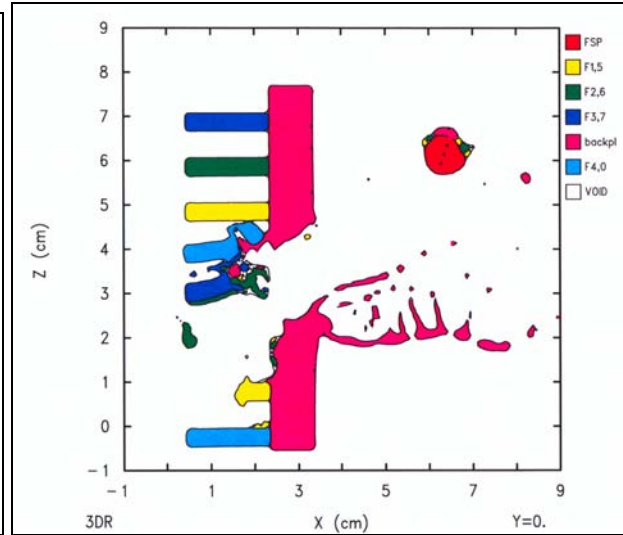


Figure 6. The impact at 280  $\mu\text{s}$  for the actual scenario.

To ascertain what difference the fins made in resisting the wall penetration, the previous simulation was repeated without the fins. Figures 8 through 12 show the time sequence of the motion of the FSP (starting from the same initial position as before) and its interaction with the 0.4-inch-thick bare wall of the electronics box (now shown in green). The FSP moves freely until it strikes the bare wall of the box at about 30  $\mu\text{s}$ . Figure 10 shows the beginning stages of penetration at 40  $\mu\text{s}$ . Figure 11 shows that the perforation has been completed well before 100  $\mu\text{s}$  and the projectile and the debris are flying freely inside the box. In the first scenario with fins, the perforation was incomplete at 100  $\mu\text{s}$ . In figure 12, we see that because of the higher residual velocity, the FSP has traveled much farther (to the edge of the computational mesh) in 200  $\mu\text{s}$  than was the case when fins were included (figure 5). Figure 13 shows that the residual velocity magnitude is now 508 m/s compared to 222 m/s for the case when fins were included

(figure 7). (It may be noted that the sudden decrease in velocity shortly after 200  $\mu\text{s}$  in figure 13 is fictitious; the FSP is merely leaving the computational mesh.) According to CTH simulations, there is no discernible mass erosion of the projectile.

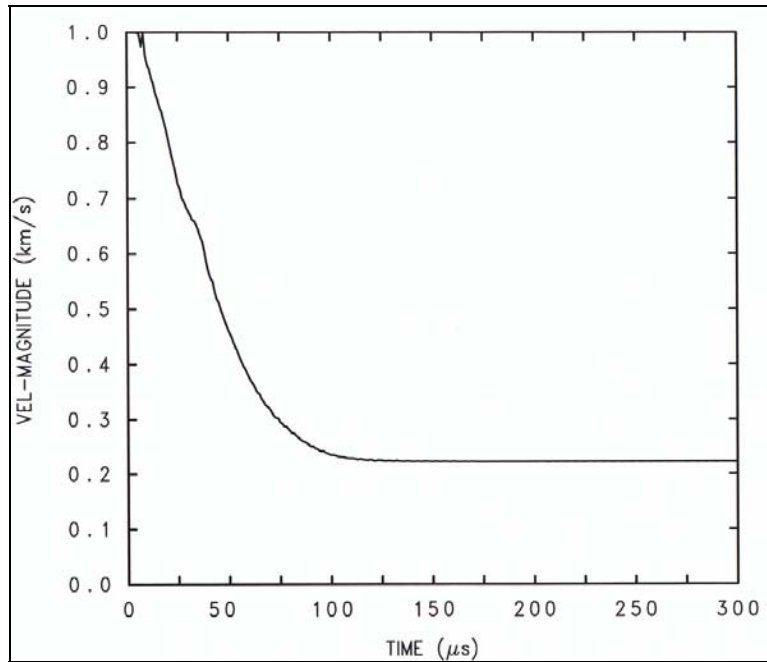


Figure 7. Projectile velocity as a function of time for the actual scenario.

For this simple scenario, THOR gives the residual velocity magnitude to be 622 m/s, and FATEPEN (version 3.0.0b) gives 504 m/s. We see that FATEPEN gives a value close to that obtained by CTH simulation without the fins, but THOR gives a value 20% in excess of that obtained by CTH. FATEPEN gives a residual mass of 2.77 g, i.e., a mass loss of 0.29 g (9%). THOR gives a residual mass of 2.68 g, i.e., a mass loss of 0.38 g (12%).

Another way to examine the penetration and generation of BAD for the case when the fins are included (section 3.1) would be to put a layer of material (aluminum) on top of the bare wall of the box to represent the fins. In the simulation of section 3.1, the FSP interacts directly with at least two fins, perhaps three (figures 3 and 4). Accordingly, CTH, THOR, and FATEPEN can be used to analyze cases when a layer of aluminum equal to two fin thicknesses is added to the bare wall and when the layer thickness is taken to be equal to three fin thicknesses.

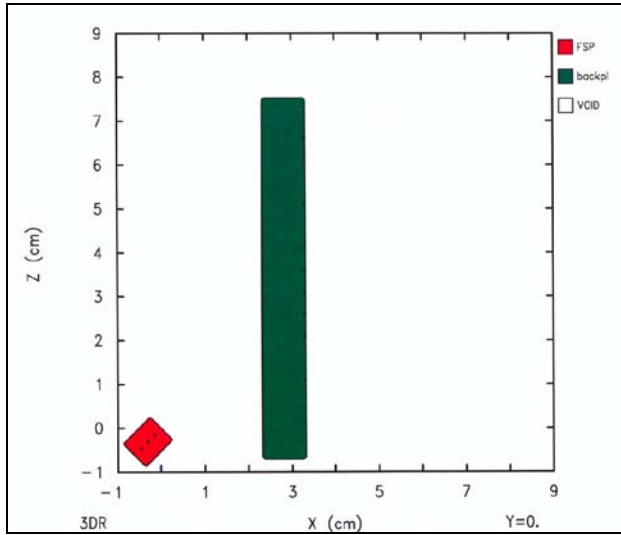


Figure 8. Initial state ( $0 \mu\text{s}$ ) of CTH simulation of oblique impact of the projectile on the bare wall without fins.

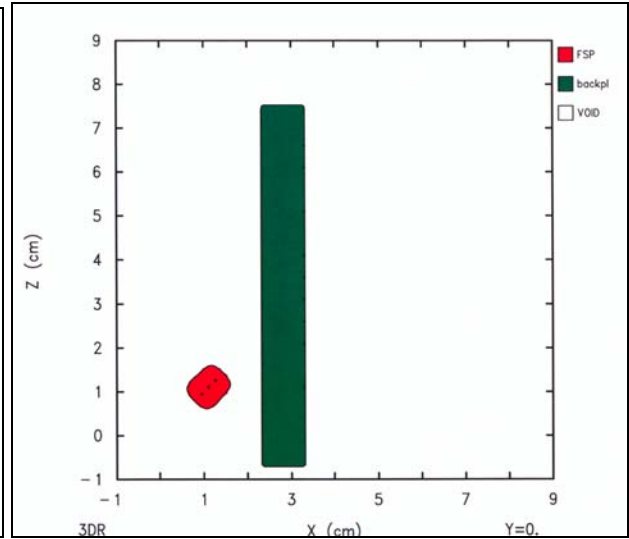


Figure 9. The simulation for the bare wall impact at  $20 \mu\text{s}$ .

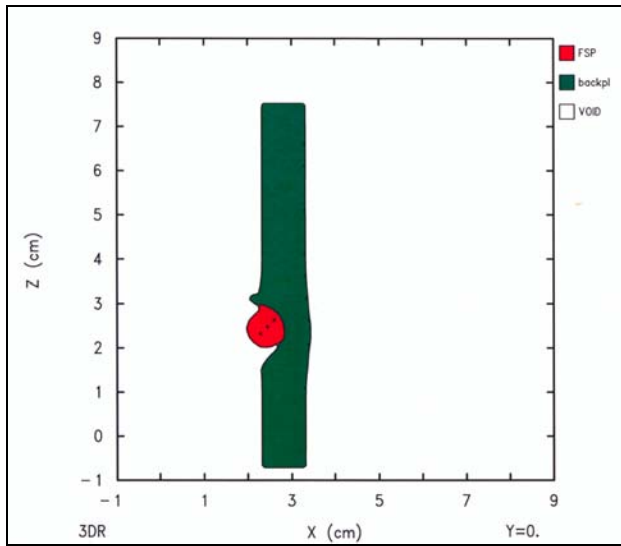


Figure 10. The simulation for the bare wall impact at  $40 \mu\text{s}$ .

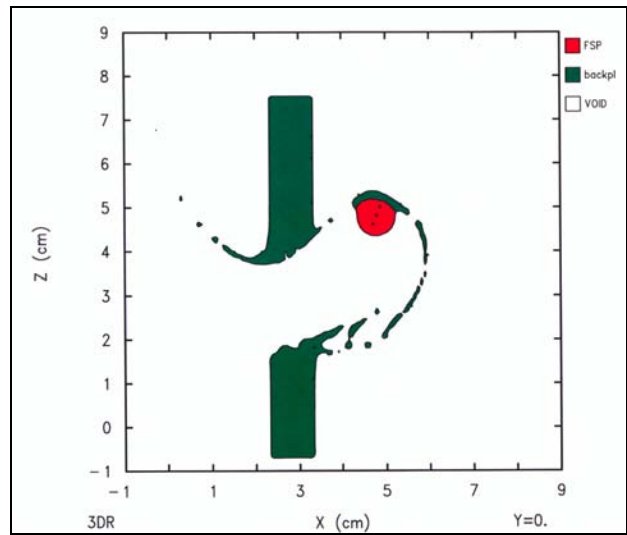


Figure 11. The simulation for the bare wall impact at  $100 \mu\text{s}$ .

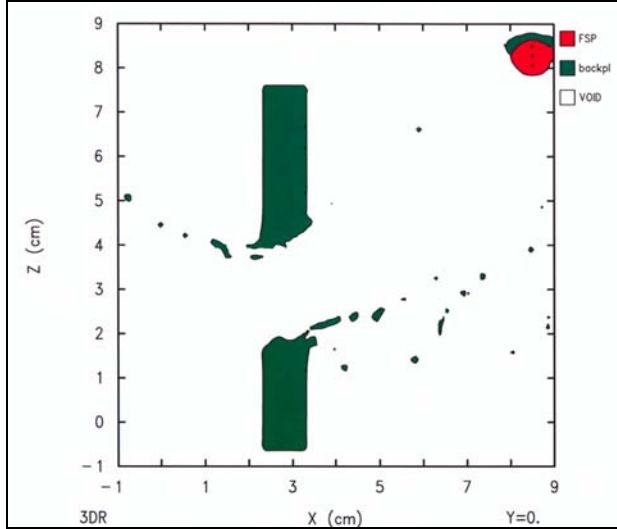


Figure 12. The simulation for the bare wall impact at 200  $\mu$ s.

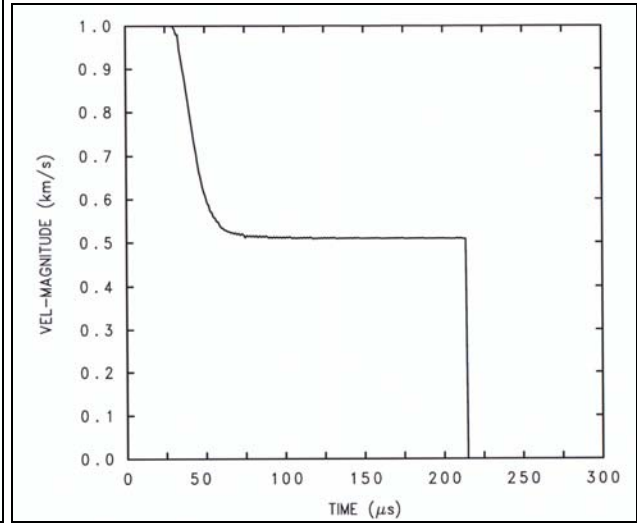


Figure 13. The simulation for the bare wall impact at 100  $\mu$ s.

### 3.3 Simulation With Walls of Equivalent Thicknesses

The results of the CTH simulation with the bare wall of the box covered with a layer equivalent to twice the fin thickness is shown in time sequence at 0  $\mu$ s, 20  $\mu$ s, 40  $\mu$ s, 100  $\mu$ s, 200  $\mu$ s, and 280  $\mu$ s in figures 14 through 19. The wall is shown in green color. From 100  $\mu$ s onward, we do see some similarity between these figures and the corresponding figures of section 3.1 (figures 4 through 6).

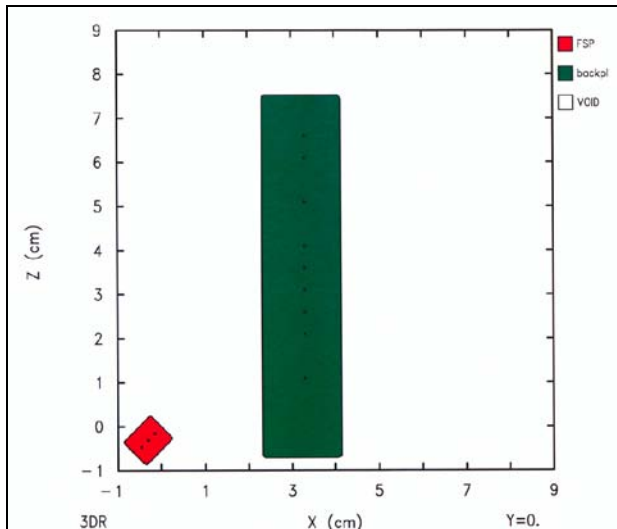


Figure 14. Initial state (0  $\mu$ s) of CTH simulation of oblique impact of the projectile on a wall of thickness equal to that of the bare wall plus the thickness of two fins.

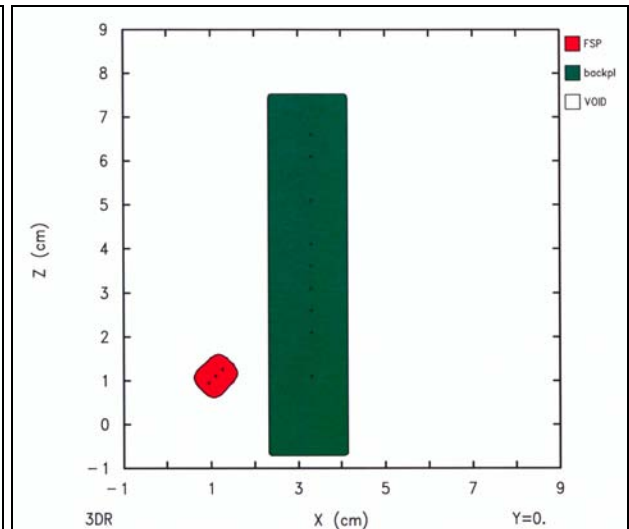


Figure 15. The simulation with wall thickness increased by twice the fin thickness at 20  $\mu$ s.

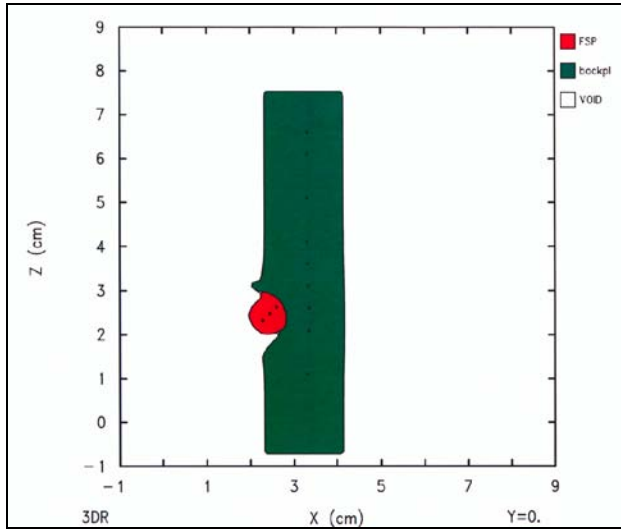


Figure 16. The simulation with wall thickness increased by twice the fin thickness at 40  $\mu$ s.

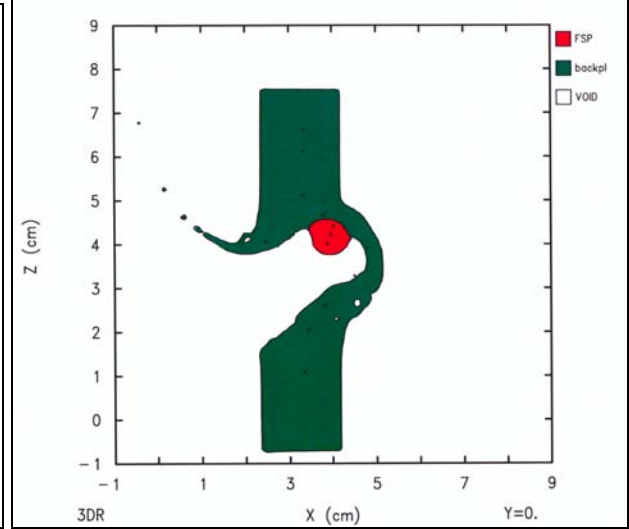


Figure 17. The simulation with wall thickness increased by twice the fin thickness at 100  $\mu$ s.

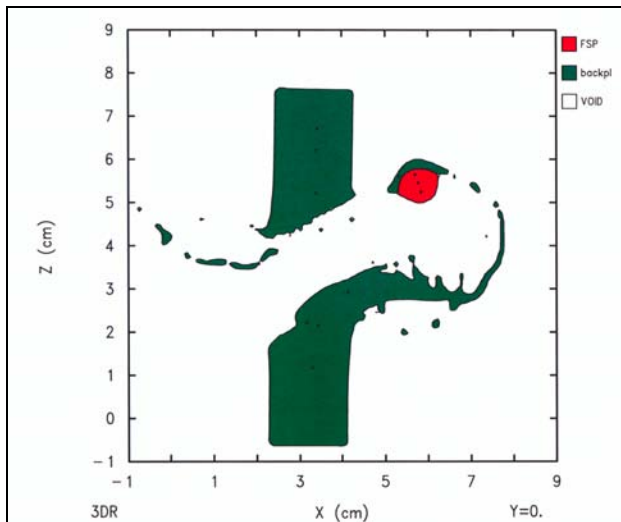


Figure 18. The simulation with wall thickness increased by twice the fin thickness at 200  $\mu$ s.

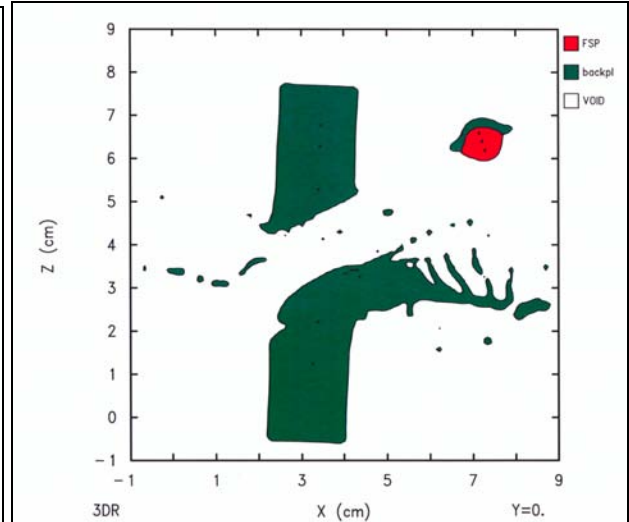


Figure 19. The simulation with wall thickness increased by twice the fin thickness at 280  $\mu$ s.

To see quantitatively the new residual velocity magnitude, the time history of the magnitude of the FSP velocity is plotted in figure 20. It is seen that the residual velocity magnitude for this adjusted bare wall thickness is 218 m/s, which is close to that obtained (222 m/s) in the CTH simulation of the actual scenario with fins. However, the direction of the residual velocity vector is slightly different. This is because the x- and z- components of velocity in the CTH simulation of section 3.1 were 174 m/s and 138 m/s, respectively, whereas now they are 184 m/s and 117 m/s, respectively. This indicates that the replacement of the fins by a layer twice the fin thickness on the wall is a close approximation but is not exactly equivalent to the actual scenario for the purpose of obtaining the residual velocity.

For the case of the bare wall to which a layer of aluminum equivalent to twice the fin thickness is added, THOR gives a residual velocity magnitude of 385 m/s, which is more than 50% larger than the residual velocity magnitude (218 m/s) obtained from the corresponding CTH simulation described before. As for FATEPEN, it shows no perforation (residual velocity of 0 m/s). According to CTH, there is no mass erosion of the FSP. FATEPEN also predicts no mass loss. However, THOR gives a residual mass of 2.62 g, i.e., a mass loss of 0.44 g (14%).

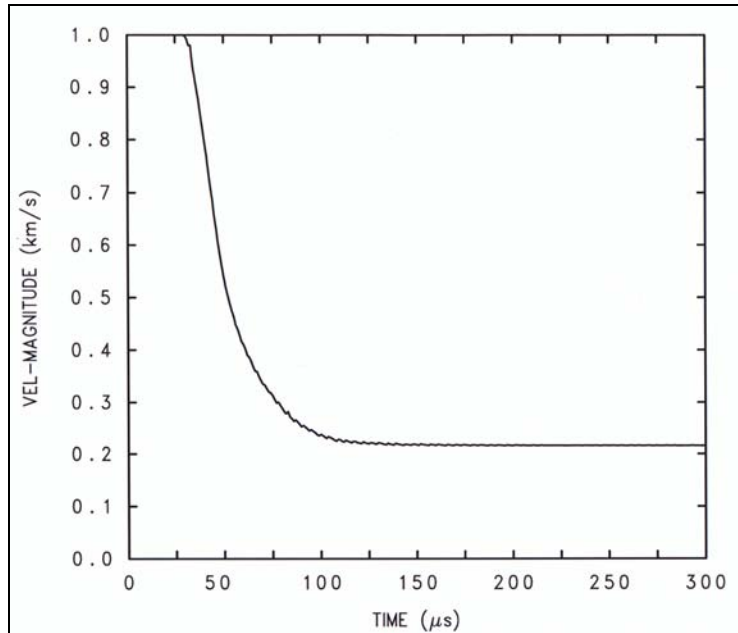


Figure 20. Projectile velocity as a function of time for the case when wall thickness is increased by twice the fin thickness.

To complete the set of simulations described at the end the last section, an additional 3-D CTH simulation was conducted with a thicker bare wall, comprised of the original wall plus a layer of aluminum of three times the fin thickness. The results are shown in time sequence 0 μs, 20 μs, 40 μs, 100 μs, 200 μs, and 280 μs in figures 21 through 26. It is seen that the FSP just manages to perforate this wall. However, CTH shows no discernible mass erosion of the projectile. To obtain a quantitative idea of the deceleration of the FSP, the magnitude of FSP velocity is plotted as a function of time in figure 27. It is seen that the FSP rapidly decelerates to attain a residual velocity magnitude of 73.8 m/s.

For this thick wall, FATEPEN does not predict any perforation (residual velocity of 0 m/s), but THOR does, with a residual velocity of 270 m/s and a residual mass of 2.60 g, i.e., a mass loss of 0.46 g. This mass loss is relatively small (15%). However, the residual velocity predicted by THOR is more than three times the predicted residual velocity obtained by the CTH simulation. The results of residual velocities for the various cases are summarized in table 1.

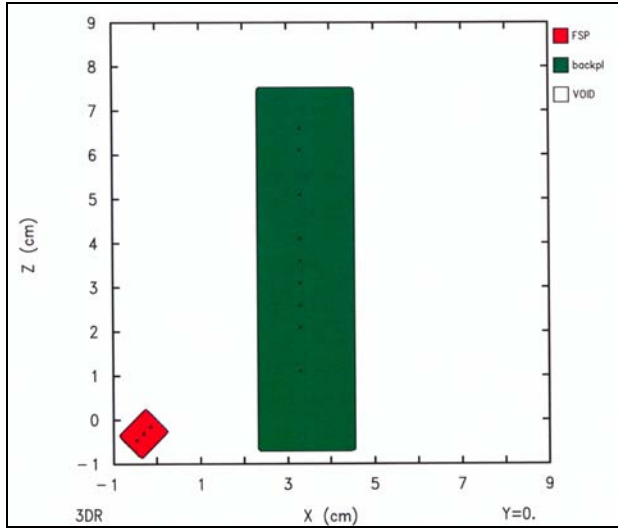


Figure 21. Initial state ( $0 \mu\text{s}$ ) of CTH simulation of oblique impact of the projectile on a wall of thickness equal to that of the bare wall plus the thickness of three fins.

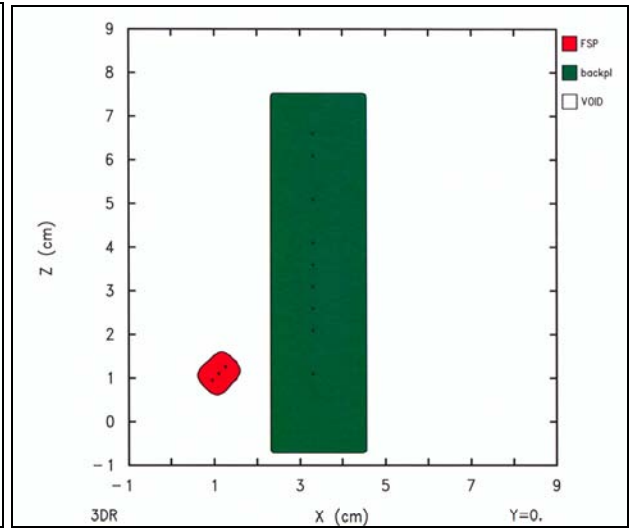


Figure 22. The simulation with wall thickness increased by three times fin thickness at  $20 \mu\text{s}$ .

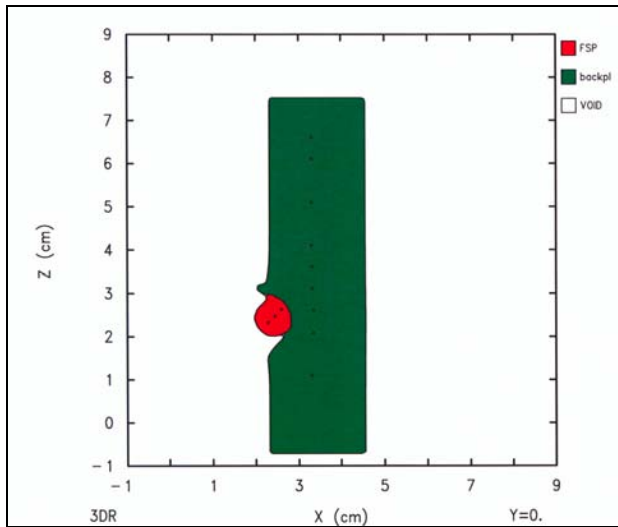


Figure 23. The simulation with wall thickness increased by three times fin thickness at  $40 \mu\text{s}$ .

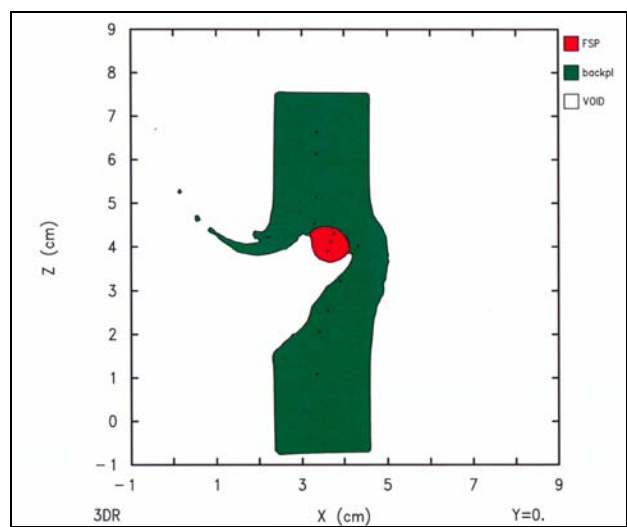


Figure 24. The simulation with wall thickness increased by three times fin thickness at  $100 \mu\text{s}$ .

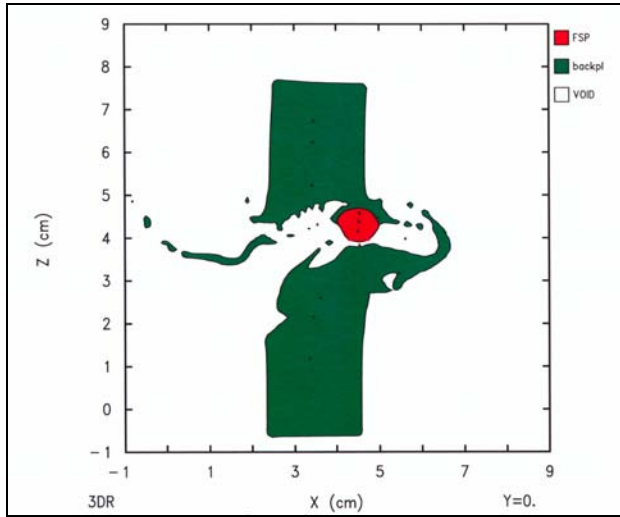


Figure 25. The simulation with wall thickness increased by three times fin thickness at 200  $\mu$ s.

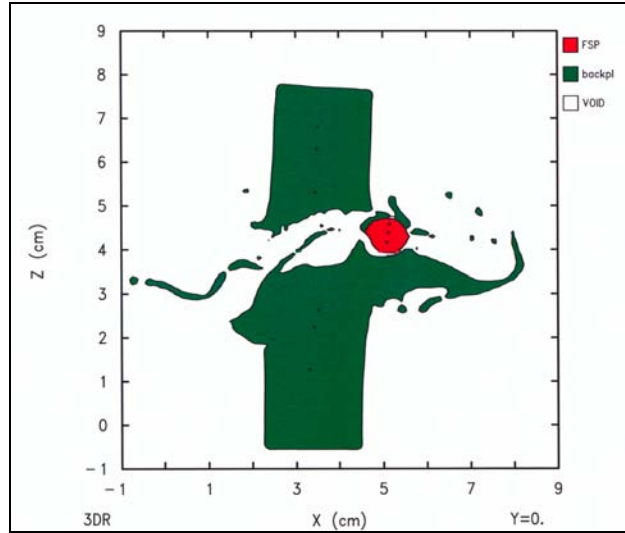


Figure 26. The simulation with wall thickness increased by three times fin thickness at 280  $\mu$ s.

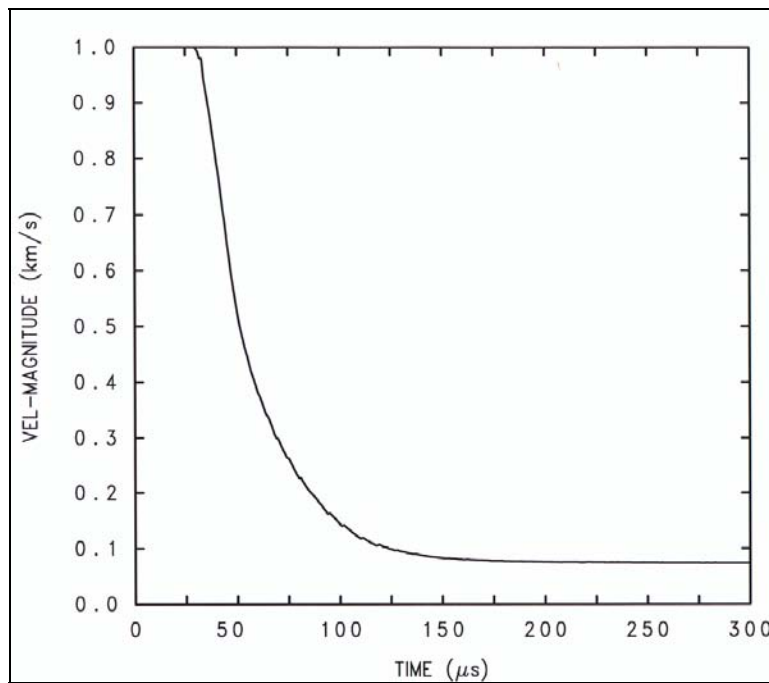


Figure 27. Projectile velocity as a function of time for the case when wall thickness is increased by three times the fin thickness.

Table 1. Summary of residual velocity magnitudes.

Wall Thickness	CTH	FATEPEN	THOR
1.02 cm (fins present)	222 m/s	N/A	N/A
1.02 cm	508 m/s	504 m/s	622 m/s
1.82 cm	218 m/s	0 m/s	385 m/s
2.23 cm	74 m/s	0 m/s	270 m/s

The reasons for these differences between the predictions of CTH, FATEPEN, and THOR are not fully understood at this time. Further investigations would be needed to identify what causes these differences. It is recommended that experiments be conducted first to validate the CTH results of table 1. In addition, one could consider using the existing experimental database that was used to develop FATEPEN and THOR to conduct CTH simulations for cases for which experimental details required for CTH input exist. If the predictions of CTH are found to be reasonable, one should look into the details of THOR and FATEPEN calculations to identify the causes of the differences in the predictions and to determine, if possible, what those differences might mean to MUVES-S2 analyses using THOR and FATEPEN.

---

## 4. Summary and Discussion

---

Physics-based 3-D simulations with the CTH hydrocode have been conducted to study the penetration into the driver's integrated display of a Stryker vehicle of a high velocity FSP impacting obliquely (at 45 degrees) on the top wall. This display is an aluminum electronics box which has vertical cooling fins on the top wall. These simulations provide details of the perforation of the FSP into this complex configuration. By conducting CTH simulations with and without the fins, we quantitatively determined the effect of fins on the residual velocity of an FSP impacting the box through the fins. The effect of fins on the residual velocity was found to be significant. Based on this result, it is recommended that future MUVES-S2 analyses involving vehicles with electronics boxes that have cooling fins should consider this detail in the geometric modeling.

We conducted more CTH simulations in which the fins were replaced by the addition of equivalent wall thicknesses. It was found that a CTH simulation with an added wall thickness equal to the thickness of two fins gave a residual velocity magnitude close to that obtained in the simulation with the actual fin geometry. Since MUVES-S2 uses the algorithms FATEPEN or THOR to calculate the residual velocity magnitude of the impacting projectile, the CTH predictions of the residual velocity magnitudes for different wall configurations were also compared with the predictions of FATEPEN and THOR.

It is only noted here that for the geometry of the thin bare wall (table 1, second row of data) without any fins, FATEPEN gives a prediction close to that of CTH. For the thicker wall (table 1, third row of data), which was found by CTH to be equivalent to the finned wall for reproducing the residual velocity magnitude, FATEPEN does not predict perforation. THOR predicts a perforation for this wall, but it gives a higher residual velocity when this velocity is compared to the CTH prediction. The higher residual velocity predicted by THOR, as compared to CTH, is also seen for the thicker wall (table 1, fourth row of data).

Although CTH code has undergone general validation testing, it is recommended that laboratory experiments of the scenarios be conducted to validate the absolute values of residual velocities predicted by CTH for the specific cases simulated here. Once the CTH predictions have been

validated, further investigations should be conducted to determine the factors responsible for differences between CTH predictions and those of FATEPEN and THOR penetration equations.

---

## 5. References

---

1. Yatteau, J. D.; Zernow, R. H.; Recht, G. W.; Edquist, K. T. *FATEPEN (Version 3.0.0b) Terminal Ballistic Penetration Model*; ARA Project 4714, Prepared for Naval Surface Warfare Center: Dahlgren, VA, Under CBDCOM Contract DAAA15-94-D-0005, D.O. 0073, January 1999.
2. Project THOR. *The Resistance of Various Metallic Materials to Perforation by Steel Fragments; Empirical Relationships for Fragment Residual Velocity and Residual Weight*; TR-47, U.S. Army Ballistics Research Laboratory, Institute for Cooperative Research, The Johns Hopkins University, April 1961.
3. McGlaun, J. M.; Thompson, S. L.; Elrick, M. G. CTH: A Three-Dimensional Shock Wave Physics Code. *Int. J. Impact Engng.* **1990**, *10*, 351-360.
4. Johnson, G. R.; Cook, W. H. A Constitutive Model and Data for Metals Subjected to Large Strains, High Strain Rates and High Temperatures. *in Proc. of the Seventh International Symposium on Ballistics*, The Hague, The Netherlands, 1983.
5. Johnson, G. R.; Cook, W. H. Fracture Characteristics of Three Metals Subjected to Various Strains, Strain Rates, Temperatures, and Pressures. *J. of Engineering Fracture Mechanics* **1985**, *1*, 31-48.
6. Grady, D. E.; Kipp, M. E. Geometric Statistics and Dynamic Fragmentation. *J. Appl. Phys.* **1985**, *58*, 1210-1222,.

INTENTIONALLY LEFT BLANK

---

## Appendix A. CTH Input Details for the Actual Scenario With the Fins

---

```
*eor* genin
anand Ff45a+ .3Cal FSP(45 deg) at 1000 ms g in al- fins- on box
control
  ep
  mmp
endc
mesh
  block 1 geom=3dr type=e
x0=-1.02254
x1 w=10. dxf=.08 dxl=.08
endx
y0=0.
y1 w=2.48 dyf=.08 dyl=.08
endy
z0=-1.02254
z1 w=10. dzf=.08 dzl=.08
endz
  xact -.96 .8
  yact 0. .8
  zact -.96 .8
endb
endm
insertion_of_material
  block 1
  package FSP
    material 1
    numsub 10
    xvelocity 7.07113e4
    zvelocity 7.07113e4
    insert cyl
  ce1 -.62254 0. -.62254
  ce2 0. 0. 0.
  rad .375
  endi
  endp
  package fin1
    material 2
    numsub 10
    insert box
  p1 .4 0. .4
  p2 2.31 4.48 .8064
  endi
  endp
  package fin2
    material 3
    numsub 10
    insert box
  p1 .4 0. 1.416
  p2 2.31 2.48 1.8224
  endi
  endp
  package fin3
  material 4
    numsub 10
    insert box
  p1 .4 0. 2.432
  p2 2.31 2.48 2.8384
  endi
  endp
  package vertbox
```

```

    material 5
    numsub 10
    insert box
    p1 2.31 0. -.72
    p2 3.326 2.48 7.52
    endi
  endp
package fin4
  material 6
  numsub 10
  insert box
  p1 .4 0. 3.448
  p2 2.31 2.48 3.8544
  endi
endp
package fin5
  material 2
  numsub 10
  insert box
  p1 .4 0. 4.4640
  p2 2.31 2.48 4.8704
  endi
endp
package fin6
  material 3
  numsub 10
  insert box
  p1 .4 0. 5.480
  p2 2.31 2.48 5.8864
  endi
endp
package fin7
  material 4
  numsub 10
  insert box
  p1 .4 0. 6.496
  p2 2.31 2.48 6.9024
  endi
endp
package fin8
  material 6
  numsub 10
  insert box
  p1 .4 0. -.6160
  p2 2.31 2.48 -.2096
  endi
endp
endb
endi
tracer
  block 1
  add -.1556 0. -.1556
  add -.3111 0. -.3111
  add -.4667 0. -.4667
  add 3.3 0. 1.1
  add 3.3 0. 2.1
  add 3.3 0. 2.6
  add 3.3 0. 3.1
  add 3.3 0. 3.6
  add 3.3 0. 4.1

```

```

add 3.3 0. 5.1
add 3.3 0. 6.1
add 3.3 0. 6.6
  endb
endt
eos
mat1 mgr '304_SS' ro=7.8724
mat2 mgrun '1100-0_AL'
mat3 mgrun '1100-0_AL'
mat4 mgrun '1100-0_AL'
mat5 mgrun '1100-0_AL'
mat6 mgrun '1100-0_AL'
ende
epdata
matep 1 jo='STEEL' tmelt=1.e10 poisson=.279
jfrac='STEEL' jfpf0=-20.e9
matep 2 jo='1100 ALUMINUM'
  poisson=.33 tmelt=1.e10
gkfrg='ALUMINUM_6061' jfpf0=-15.e9
matep 3 jo='1100 ALUMINUM'
  poisson=.33 tmelt=1.e10
gkfrg='ALUMINUM_6061' jfpf0=-15.e9
matep 4 jo='1100 ALUMINUM'
  poisson=.33 tmelt=1.e10
gkfrg='ALUMINUM_6061' jfpf0=-15.e9
matep 5 jo='1100 ALUMINUM'
  poisson=.33 tmelt=1.e10
gkfrg='ALUMINUM_6061' jfpf0=-15.e9
matep 6 jo='1100 ALUMINUM'
  poisson=.33 tmelt=1.e10
gkfrg='ALUMINUM_6061' jfpf0=-15.e9
  mix 3
ende
*eor* cthin
anand Ff45a+ fsp(45 deg) 1000ms g in al- fin-
fracts
  pressure
pfrac1 -20.e9
pfrac2 -15.e9
pfrac3 -15.e9
pfrac4 -15.e9
pfrac5 -15.e9
pfrac6 -15.e9
pfmix -1.e20
pfvoid -1.e20
endf
control
tstop=400.e-6
endc
cellthermo
mmp
ntbad=999999
endc
convt
convection=1
interface=high
endc
edit
  shortt
    time=0. dt=10.e-6

```

```
ends
longt
  time=0. dt=200.e-6
endl
plott
  time=0. dt=5.e-6
endp
histt
  time=0. dt=10.e-7
  htracers all
endh
ende
boundary
  bhydro
    block 1
      bxbot=1
      bxtop=1
      bybot=0
      bytop=1
      bzbot=1
      bztop=2
    endb
  endh
endb
```

NO. OF  
COPIES ORGANIZATION

- \* ADMINISTRATOR  
DEFENSE TECHNICAL INFO CTR  
ATTN DTIC OCA  
8725 JOHN J KINGMAN RD STE 0944  
FT BELVOIR VA 22060-6218  
\*pdf file only
- 1 DIRECTOR  
US ARMY RSCH LABORATORY  
ATTN IMNE ALC IMS MAIL & REC MGMT  
2800 POWDER MILL RD  
ADELPHI MD 20783-1197
- 1 DIRECTOR  
US ARMY RSCH LABORATORY  
ATTN AMSRD ARL CI OK TL TECH LIB  
2800 POWDER MILL RD  
ADELPHI MD 20783-1197
- 1 DIRECTOR  
US ARMY RSCH LABORATORY  
ATTN AMSRD ARL SL ES J GONZALEZ  
BLDG 1648  
WSMR NM 88002-5513

ABERDEEN PROVING GROUND

- 1 DIRECTOR  
US ARMY RSCH LABORATORY  
ATTN AMSRD ARL CI OK (TECH LIB)  
BLDG 4600
- 2 US ARMY RESEARCH LAB  
ATTN AMSRD ARL SL P TANENBAUM  
J BEILFUSS  
BLDG 328
- 3 US ARMY RESEARCH LAB  
ATTN AMSRD ARL SL B D BELY  
J FRANZ M PERRY  
BLDG 328
- 7 DIRECTOR  
US ARMY RSCH LABORATORY  
ATTN AMSRD ARL SL BB S JUARASCIO  
D FARENWALD R DIBELKA  
G KUCINSKI P KUSS  
J PLOSKONKA W WINNER  
BLDG 328
- 1 US ARMY RESEARCH LAB  
ATTN AMSRD ARL SL BD R GROTE  
BLDG 1068

NO. OF  
COPIES ORGANIZATION

- 7 US ARMY RESEARCH LAB  
ATTN AMSRD ARL SL BE L ROACH  
A PRAKASH (5 CYS) R SAUCIER  
BLDG 328
- 1 US ARMY RESEARCH LAB  
ATTN AMSRD ARL SL E M STARKS  
BLDG 328
- 1 US ARMY RESEARCH LAB  
ATTN AMSRD ARL SL EC J FEENEY  
BLDG 328
- 1 US ARMY RESEARCH LAB  
ATTN AMSRD ARL SL EM D BAYLOR  
BLDG 328